

# Carrier leakage in Ge/Si core-shell nanocrystals for lasers: core size and strain effects

Mahesh R. Neupane<sup>a</sup>, Rajib Rahman<sup>b</sup>, and Roger K. Lake<sup>a</sup>

<sup>a</sup>Department of Electrical Engineering, University of California, Riverside, CA 92521-0204

<sup>b</sup>Sandia National Laboratories, Albuquerque, NM 87185

## ABSTRACT

The electronic structure and optical properties of Ge/Si quantum dot (QD) were investigated using the atomistic tight binding method as implemented in NEMO3D. The thermionic lifetimes that govern the hole current leakage mechanism in the Ge/Si QD based laser, as a function of the Ge-core size and strain is also calculated by capturing the bound and extended eigenstates, well below the band edges. We also calculated, the effect of both core size variation and strain on oscillator strengths, transition energy and transition rates. Finally, the quantitative and qualitative analysis of leakage current, due to the thermionic emission, and temperature sensitive characteristics is presented.

**Keywords:** Ge/Si QD, Laser, oscillator strength, thermionic lifetime, leakage current

## 1. INTRODUCTION

A quantum dot (QD) laser is a semiconductor laser in which electrons and holes are injected from 3D contact regions, where carriers are free, into an active region with QDs, where lasing transition take place and carriers are confined in all directions. The main motivation behind the idea of a QD laser was to conceive a design for a low-threshold, single-frequency, and temperature-insensitive laser due to the quantum confinement effect. Ge/Si core-shell (Type-II heterostructure) QD laser has been proposed due to its capability to use existing Si based fabrication scheme and exhibiting size dependent stimulated emission.<sup>1</sup> Recent experimental reports also suggested in increase in the light emission probability of such laser by increasing radiative lifetimes due to an extra Si-shell layer around Ge QD acting as an auxiliary quantum well (QW) coupled to the quantum dots by tunneling via a thin barrier and hence, suppressing the carrier leakage current.<sup>2</sup> This structure overcomes the limitations of carrier collection, lateral transport, and thermalization of the quantum dots. The carrier (hole) current leakage mechanism in Ge/Si core-shell QD is governed by thermionic lifetime of the confined carrier in the Ge-core region. Thermionic barrier height is a key parameter that governs the thermionic emission mechanism, which is calculated by finding the difference between the energy levels. Depending on the core/shell size, the barrier heights for electrons and holes can be varied independently. This tunability nature of the barrier height allows the optimization of the structure by minimizing thermal emission, a fundamental operational requirement for the QD based lasing device.<sup>3</sup>

Several photoluminescence studies have been carried out extensively on the Ge/Si quantum dots while observing the electroluminescence of Ge quantum dots at room temperature in the spectral region around 1.31.5  $\mu\text{m}$ . Despite the recent progress in controlling QD parameters such as size and strain during growth, significant QD size dispersion, as indicated by the measured gain and spontaneous emission spectra, has been observed and need for the large scale atomistic study has been sought after. Similarly, analysis of core/shell-size and strain effect in Ge/Si QD laser, using atomistic tight binding simulation, on optical, electronic properties, leakage current, and temperature sensitivity characteristics on the overall performance is lacking.

In this work, we carry out a computational study of the low-energy electronic states in Ge/Si core-shell QD laser using a full-band,  $\text{sp}^3\text{d}^5\text{s}^*$  model implemented in NEMO3D.<sup>4</sup> Valence Force Field (VFF) model is used to determine the strain distribution in the Ge-core/Si-shell QD and strain contribution to the optical

---

Further author information: (Send correspondence to Mahesh Raj Neupane)  
Mahesh Raj Neupane: E-mail: mneup001@ucr.edu, Telephone: 1 951 640 2383

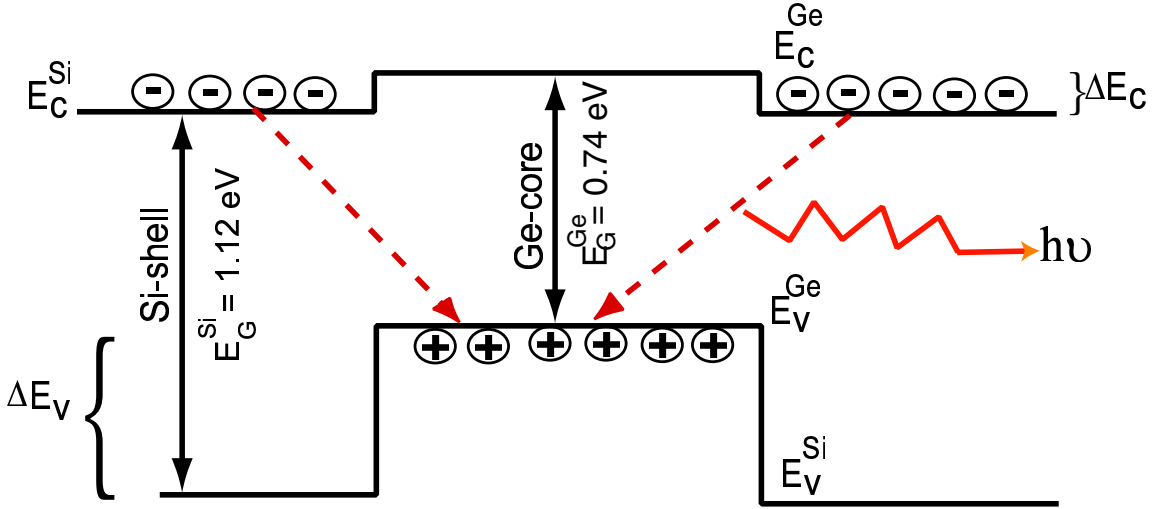


Figure 1. (Color online) Energy diagram and wave function distribution in the Ge/Si core-shell NC. The offsets shown in the band edges correspond to the bulk Si and Ge parameters used in the calculations. Confinement will alter the position of the energy levels. Dashed lines show the e-hole recombination mechanism.

properties. This is particularly important for strained systems such as QD heterostructure since the conduction band and valence band cannot be decoupled in the presence of large strain fields. Barrier heights and decay constants, required for the leakage current and threshold current formulation, are determined from the calculated energy levels and corresponding wavefunctions. In addition, a solution to decrease the threshold current by modulating the Ge-core size on strain compensated Si-shell is presented.

## 2. THEORY AND MODEL

### 2.1 Electronic Properties

Bulk Ge and Si when joined together form a Type-II heterojunction,<sup>5</sup> in which electrons and holes are spatially separated between the shell and the core region respectively and hence, the hole life time in the core region increases due to the minimal electron-hole recombination.<sup>5</sup> The type-II band lineup between Ge and Si in Ge/Si QD and the large valence band offset leads to an effective confinement of holes in the Ge region while electrons are mostly presented in the Si layers. This lead to the enhancement of oscillator strength of the optical interband transition. Because of the indirect nature of the band gap of Ge/Si system, the overall dot size or Ge core size should be tuned to observe the photoresponse to the desirable spectral region. Fig.1 shows the bulk band alignment between Ge and Si and carrier excitation and localization. The electronic states are modeled using the  $sp^3d^5s^*$ , nearest-neighbor, empirical-tight-binding model with spin-orbit(SO) coupling as implemented in NEMO3D and described in Ref.<sup>6</sup> The strain effect is calculated using Valence Force Field (VFF) method with the Keating potential modified to include anharmonic corrections.<sup>7</sup> The VFF model is a microscopic theory that includes bond stretching and bond bending, and avoids the potential failure of elastic continuum theory in the microscopic limit. The strain domain has free boundary conditions in all directions, whereas the electronic domain has closed boundary condition. The energies of the dangling bonds at the surface are shifted by 20 eV so that the effect of the dangling bonds on the density of states near the bandgap is negligible.<sup>8</sup>

The eigenvalues and eigenstates are solved using a Lanczos algorithm. This model and implementation in NEMO3D has proven its reliability in predicting the electronic properties of nano-structures.<sup>9</sup> One of the simulated structures with a Ge core diameter of 2 nm is shown in Fig.2. Free-standing spherical Ge/Si core-shell NCs with core diameters ranging from 1-4 nm are considered. The thickness of the Si shell is maintained at 5 nm around the Ge core region. The strain is applied at the Ge/Si interface. The inter-band optical transition strengths are calculated using Fermi's golden rule as the squared magnitude of the momentum matrix elements summed over the spin degenerate states.

## 2.2 Optical Properties

Electronic parameters obtained for Ge/Si core-shell structure, a separate confinement heterostructure (SCH) laser, using tight binding method are used to calculate various optical properties, such as intersubband transition rate, oscillator strength, overlap integrals, momentum matrix element (MME) and absorption coefficient.

The oscillator strength is a very important physical quantity in the study of the luminescence properties of any optical device which are related to the electronic dipole-allowed transition. The concentration of oscillator strength in discrete energy levels of QDs make QDs a promising candidate for electro-optic and nonlinear optical application in the future device technology. It's amplitude depends on the light polarization directions in accordance with the coordinate axes i.e. x,y and z, and should be equal due to the symmetric/spherical nature of the calculated atomic structures. Generally, the oscillator strength  $OS_{if}$  is defined as,

$$OS_{if} = \frac{2}{m_w^* \hbar \omega_{if}} \|M_{if}\|^2 \quad (1)$$

where  $m_w^*$  is the effective mass in the Ge-core region,  $\hbar \omega_{if} = \Delta E_{if} = E_i - E_f$ , where  $E_i$  and  $E_f$  are the energy levels of the initial  $|i\rangle$  and final  $|f\rangle$  electronic states and  $\|M_{if}\|$ , in the electric dipole approximation, the dipole induced MME between the initial ( $|i\rangle$ ) and final state ( $|f\rangle$ ) is given by,

$$\|M_{if}\| = \langle \psi_i^*(x, y, z) | e(x, y, z) | \psi_f(x, y, z) \rangle \quad (2)$$

where  $\langle \psi_i$  and  $|\psi_f(x, y, z)\rangle$  are the wave functions of initial and final states. The required transition rate ( $\Gamma_{if}^0$ ) between these states are strongly dependent on the MME as given in Eq.2,

$$\Gamma_{if}^0 = \frac{2\pi e^2 A^2}{\hbar 4m_0^2} \|M_{if}\|^2 \delta(E_f - E_i + E) \quad (3)$$

where  $e, A$ , and  $\hbar$  are electron charge, surface area, and reduced Plank's constant, respectively. In a QD laser, the gain is effected by not only the density of states but also the of the reduction in the optical MME<sup>7</sup>. This reduction leads to the inefficient lasing from the ground state due to the reduced overlap between the hole and electron wave functions. However, recent theoretical studies predicted that the magnitude of the MME could be engineered in order to optimize the optical gain in QD lasers and optical amplifiers.<sup>10</sup>

Similarly, achieving low threshold current is one of the fundamental requirement of QD based SCH laser. Carrier leakage processes are shown experimentally as one of the factors contribution due to the temperature sensitivity, and hence low threshold current density at room temperature. This is mainly due to the strong carrier confinement in the active region, optical confinement due to the abrupt change in the refractive index, and low carrier leakage. Higher material gain due to the reduction in the hole-leakage process in the Type-II SCH was reported earlier.[APL 86, 071116, 2005]. In order to analyze the leakage due to the heavy hole escape mechanism in the Ge/Si core-shell QD laser, we calculate the thermionic escape times of holes from the Ge-core region. The thermionic emission lifetime ( $\tau_h^{th}$ ) is determined by the height of the barrier over which the hole is emitted, and it is approximated using the expression derived by Schneider and von Klitzing.<sup>11</sup> The minimal thermionic carrier escape out of the QW will lead to an increase in the injection efficiency and the temperature sensitivity. The thermionic leakage current from the edge of the single QW to either side of the barrier is related to the thermionic emission lifetime ( $\tau_h^{th}$ ) as follows,<sup>2</sup>

$$J_h = \frac{N q W}{\tau_h^{th}} \quad (4)$$

where, N, q, W and  $\tau_h^{th}$  represents the electron charge, Ge-core size, current density and therimioinc emission carrier lifetime. The current density (N) is estimated using Boltzman's Statistics at constant fermi energy level.  $\tau_h^{th}$  is defined as,<sup>12</sup>

$$\tau_h^{th} = W \sqrt{\frac{2\pi m_w^*}{k_B T}} \exp\left(\frac{\Phi_b}{k_B T}\right) \quad (5)$$

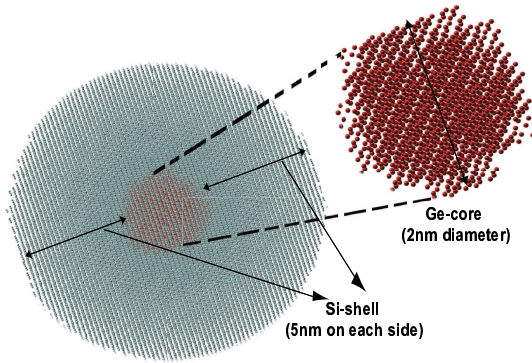


Figure 2. (Color online) Ge/Si core-shell NC (2 nm Ge core and 5nm Si-shell around Ge core). Total number atoms is 41761 (41649 Si atoms and 112 Ge atoms). The lighter gray dots are Si atoms and darker (red) dots are Ge atoms.

where,  $h$  is the Plank's constant,  $m_w^*$  is the effective mass of the hole in the Ge core,  $k_B$  is Boltzmann's constant, and  $\Phi_b$  is the potential barrier height. The potential barrier height is calculated from the energy difference between the localized ground and delocalized state of the hole,<sup>12</sup>

$$\Phi_b = E_0 - E_n. \quad (6)$$

where,  $E_0$  is the ground state hole energy and  $E_n$  is the highest energy of the hole state that does not exponentially decay in the Si shell, i.e. it is delocalized throughout the Ge/Si NC, where the quantum number  $n$  varies depending on the size of the Ge core.

### 3. RESULTS AND DISCUSSION

The calculated electronic properties, using theory presented in the section 2, is presented and analyzed in this section. In addition, results from the optical properties calculations is presented, and analyzed for Ge/Si core-shell SCH laser. At last, the hole leakage current from a single Ge/Si QD, due to the thermal excitation at room temperature, is presented.

#### 3.1 Electronic Parameters

##### 3.1.1 Energy Gap and Barrier height

Fig. 2 shows one of the simulated structures with a Ge core diameter of 2 nm. Free-standing spherical Ge/Si core-shell NCs with core diameters ranging from 1-4 nm are considered. The thickness of the Si shell is maintained at 5 nm around the Ge core region. Like in the bulk samples, strained Si/Ge QD have higher valence band offset. However, the residual interfacial strain essentially modifies band offsets. Because of larger lattice constant, Ge-core region experiences compressive strain, while a tensile strain is induced in Si-shell. As shown in the Fig.3, strain tend to shift the valence band edge by few meV for increasing core size. Consequently, the bandgap decreases due to the strain and core size. Size effect and strain effect is prominent in the valence band maxima while conduction band minima is close to constant. However, conduction band minima remains virtually constant, as expected, due to the TYPE-II heterojunction between Ge and Si. Hence, shifting of the valence band, with increasing core size and applied strain, is responsible for the band offset (barrier height) fluctuation. The barrier height ( $\Phi_b$ ), along with temperature, is one of the key parameters during the thermionic leakage current using Eq. 4.

In earlier works,<sup>13,14</sup> the barrier height was formulated by calculating the difference between the bulk valence band edge of Si and Ge. In our approach, the finite barrier height  $\Phi_b$  is calculated by taking the energy difference between the ground state energy of the hole and the delocalized state using Eq. 6. In order to correctly identify the delocalized state, a large number of excited states are calculated and analyzed. Plots of  $|\psi_0|^2$  and  $|\psi_n|^2$  are shown in the Fig. 4 for a 2 nm Ge core without strain. The energy of  $|\psi_n|^2$  defines the top of the barrier for thermionic emission of holes.

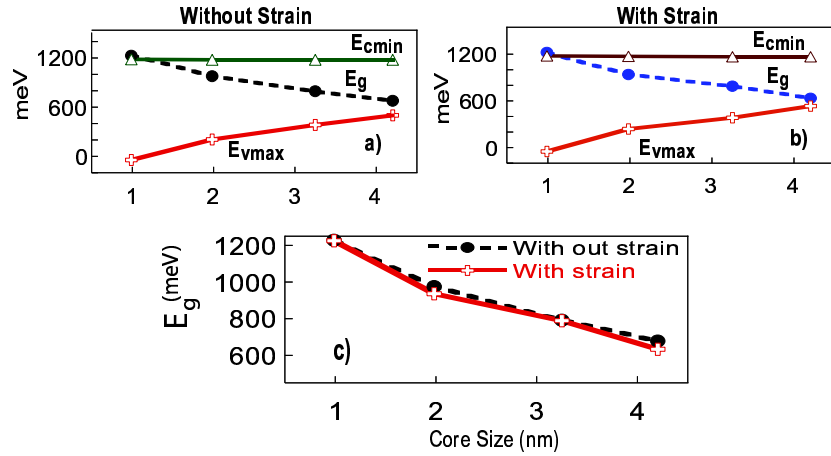


Figure 3. (Color online) a) Maximum Valence ( $E_{vmax}$ ) and Conduction band edge ( $E_{cmin}$ ) and Minimum energy gap ( $E_g$ ) without strain b) Minimum Valence and Conduction band edge and Minimum energy gap ( $E_g$ ) with strain, and c) Comparison between minimum energy gaps with and without strain, as a function of the Ge core size (nm) with a fixed 5 nm Si shell.

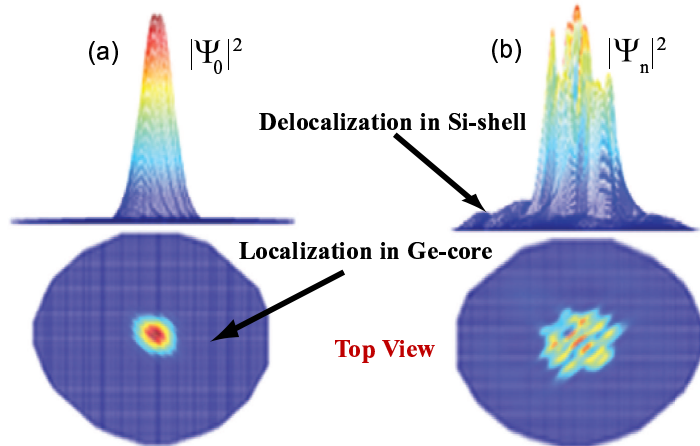


Figure 4. (Color online) Magnitude of the wavefunctions squared plotted for (a) the highest localized state and (b) the highest delocalized state in the unstrained Si(5 nm)-Ge(2 nm)-Si(5 nm) NC. The values are taken from a two-dimensional slice through the center of the NC. In this case,  $n = 8$ .

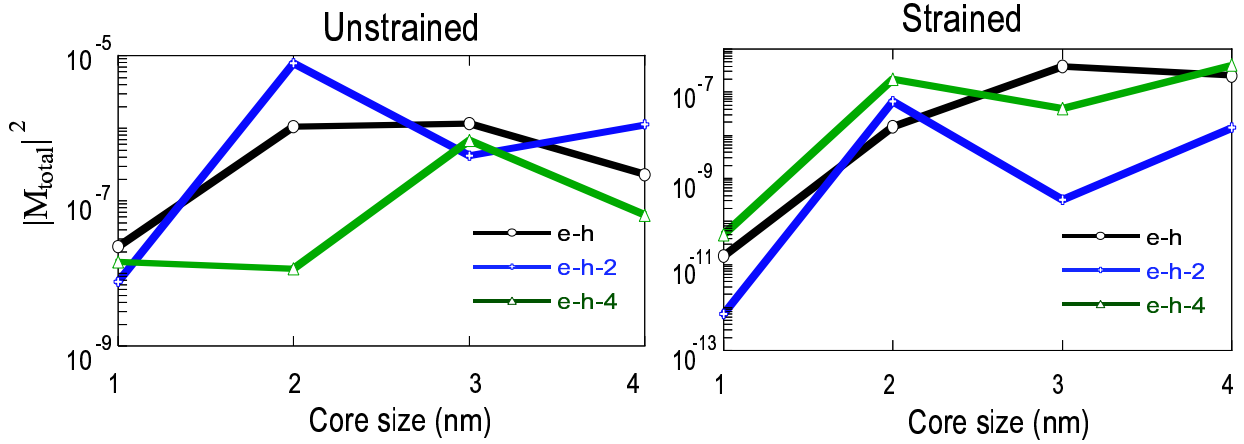


Figure 5. (Color online) Magnitude of the modulus squared of the optical matrix element  $|M_{total}|^2$  plotted against (a) the Ge-core size (b) the energy levels (from the HOMO level). The units for  $|M_{total}|^2$  is given in eV/c, where c is speed of light.

### 3.2 Optical Properties

An intersubband transition in the Ge/Si QD based laser has unique properties such as large dipole moment, relaxation time of nanoseconds, large tunability of the transition wavelength, which are obtained by choosing suitable parameters,<sup>15</sup> such as external field, strain and core-size. With external field set to zero, strain and core-size are responsible for in the electron and hole energy level fluctuation and wave function localization characteristics, and consequently, impact the transition energies and oscillator strengths within the active region of the laser.

#### 3.2.1 Momentum Matrix Elements (MME)

Optical momentum matrix for electron ground state to the highest six hole states are calculated using Eq. 2. Due to the spherical symmetry of QDs, the light polarization along the x-direction is considered. In order to understand the qualitative behavior of the MME, as it applies to the gain calculation, we consider the quantity  $|M_{total}^2|$ , which is the modulus squared of the MME for the electron hole ground state transition summed over degenerate spin states. Fig. 5 shows the calculated  $|M_{total}^2|$  with both the Ge-core size and the energy level variation only for the light polarized along the x-direction. Since the shape of the quantum dots considered here is spherically symmetric with the aspect ratios of unity, the matrix elements for each light polarized direction( x,y or z) should be equivalent. As evident from the Fig. 5,  $|M_{total}^2|$  initially increases with the core size for each transitions before reaching a peak value beyond which it decreases rapidly. The magnitude of the matrix element for smaller core size, when the isotropic strain is applied to the Ge/Si heterostructure QDs, increases by the factor of three because of the increased overlap integral between electrons and holes due to increased quantum confinement effect. However for the larger core size, the strain has no or minimal effect in the matrix element mainly due to the increased localization of the holes in the Ge-core region and electrons in the Si-shell region.<sup>10</sup>

#### 3.2.2 Interband Energies and Transitions

The transition energies is calculated by taking the difference between eigen energies of corresponding electron and hole states. Photon energies emitted by the ground state electron during the transition to the first few hole states is plotted in Fig. 6. The strain, as expected, shifts the hole energy states by reducing the required emitted photon energies. Eventually, when the core-size increases beyond the 3nm, bulk-like behavior becomes dominant and required transition energies decreases with increasing core-size, in accord with the behavior predicted for finite potential well system. Similarly, the interband transition rate between electron and hole states is calculated using the modulus squared of the optical matrix element of electron and hole states transition summed over the degenerate spin states using the Eq.3 and plotted in Fig.7. Since the shape of the quantum dots considered here is spherically symmetric and have aspect ratios of unity, the transitions of ground electron to the hole states for

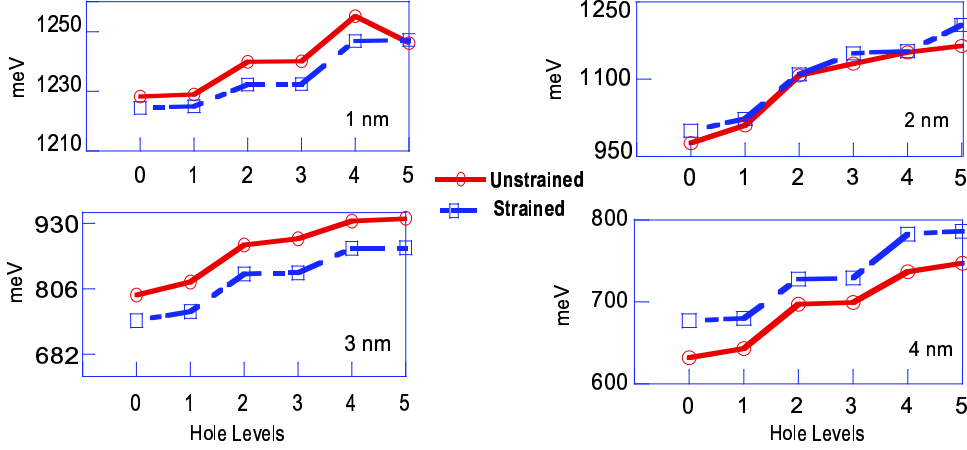


Figure 6. (Color online) Transition energies ( $\Delta E$ ), in meV, between GS electron level and first six holes states, as a function of strain and the Ge core size (nm) with a fixed 5 nm Si shell.

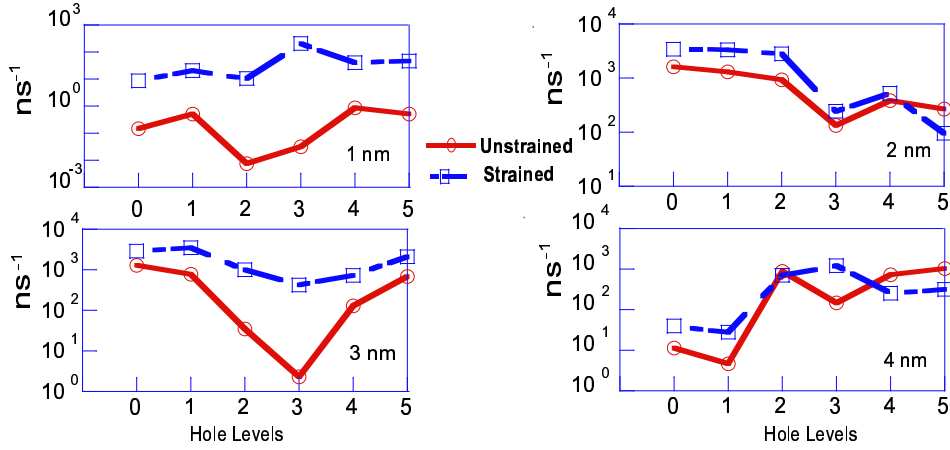


Figure 7. (Color online) Transition rates between GS electron level and first six holes states, as a function of strain and the Ge core size (nm) with a fixed 5 nm Si shell.

each light polarized direction should be equivalent. In the transition rates for Ge/Si QD's with different Ge-core sizes, when strain is included, is higher than the unstrained counterparts due to the observed shifting of the hole energy states.

### 3.2.3 Oscillator Strength

The Oscillator strength for the transitions from ground state electron to the first five hole states are for the Ge-core size is calculated using Eq.1. Fig.8 shows the oscillator strength,  $OS_{if}$ , for a range of Ge-core size from 1 nm to 4 nm for light polarized in the x-direction. The oscillator strength mainly depends on two parameters: energy difference between initial and final state and the momentum matrix element, which reflects the wavefunction overlapping between states. As can be seen from Fig.8(a), the oscillator strength is increases with the core size and reaches maximum values at 3 nm and beyond that it reaches a characteristics constant value for both strained and unstrained conditions. In small Ge-core size, the energy difference ( $\hbar\omega$ ) between electron ground state (E0) and Hole ground state (H0) is high, the overlapping between the electron and hole wavefunctions is small, i.e. the momentum matrix element ( $\|M\|^2$ ) is small. When the Ge-core size increases, the  $\|M\|^2$  increases, while the energy difference ( $\hbar\omega$ ) decreases. However, the overall effect remains constant, and hence the  $OS_{if}$  remains constant. The characteristics is in good agreement with the published results for other materials,<sup>16–18</sup> which seems to be characteristic of the transition and has approximately the same value for various investigated QD.

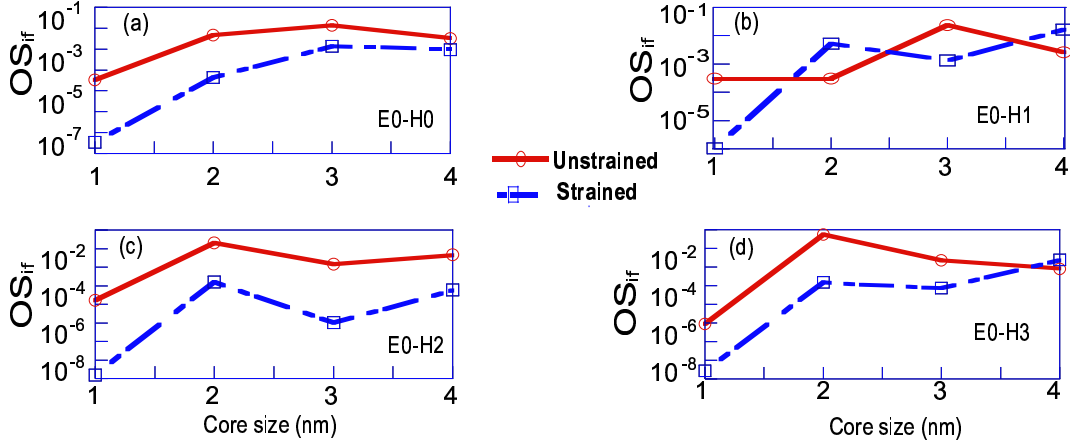


Figure 8. (Color online) Magnitude of Oscillator strength ( $OS_{if}$ ) as a function of Ge-core size and strain for the electron ground state (E0) to a) Hole ground state (H0) b) First excited hole state (H1) c) Second excited hole state (H2), and Third excited hole state (H3).

### 3.2.4 Thermionic Hole Lifetime and Leakage Current

The thermionic lifetime due to the thermionic emission from the Ge/Si QD as SCH laser is calculated for Ge-core size of 1 to 4 nm, using Eq. 5. Consequently, calculated thermionic lifetime values then used to calculate the thermal leakage current using Eq. 4. Fig. 9 illustrates the thermionic lifetime and current densities dependence on the temperature, core size and strain. At 1 nm core size, the lifetimes remain constant at different temperatures because of its dependence on energy barrier height, which is negligible at this core core size. In addition, due to the small number of Ge atoms, the strain has little impact on lifetime and carrier densities. However at larger core size, these barrier dependent parameters varies exponentially from low temperature to higher temperature. Since the energy barrier height increases with the core size,<sup>12</sup> the lifetimes, at around room temperature, varies by several orders of magnitude while varying from 1 nm to 4 nm. In addition, when strain is included in the barrier height calculation, the thermionic lifetime increases by a order of magnitude, owing it to the valence band shift.

Similarly, the leakage current density also shows the exponential dependence on increasing core size. Due to the significantly smaller  $\tau_h^{th}$  ( 1 ps) at room temperature, the leakage current for 2 nm core size, for unstrained Ge/Si QD, is around  $10 \text{ mA/cm}^2$ . Whereas, when strain is applied, the leakage current decreases by three orders of magnitude. However, when the temperature increases beyond room temperature, the thermal energy becomes larger than the energy barrier and hence, leakage current is linear and constant.

## 4. CONCLUSION

The electronic properties of Ge-core/Si-shell NCs are calculated for a fixed 5nm Si shell and Ge-cores ranging from 1 nm - 4 nm diameters. Calculations are performed atomistically using a nearest-neighbor,  $sp^3d^5s^*$  tight-binding model as implemented in NEMO3D with and without strain. The electron-hole wavefunctions and wave vectors are then used to calculate Momentum Matrix Element, Oscillator strength, Transition rates using Fermi's Golden rule. The ground state momentum matrix elements, transition energies and transition rates are less sensitive to the core-size and strain. However, the oscillator strength shows the exponential dependence on the smaller core sizes ( $\leq 3 \text{ nm}$ ) and strain due to the prominent quantum confinement effect.

The calculated thermionic emission and leakage current, at room temperature, shows exponential dependence with the temperature, core-size and strain. The leakage current reduces by eight order of magnitude when core size is increased from 2 nm to 4 nm, for both strained and unstrained conditions.

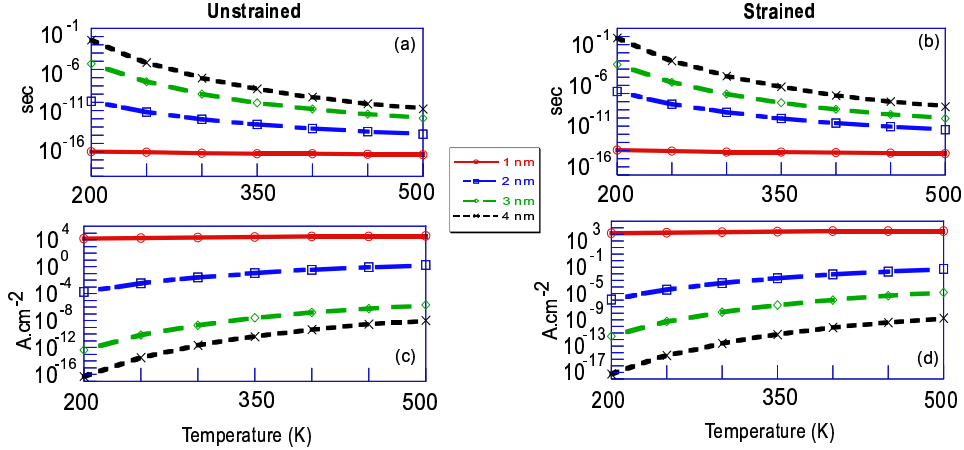


Figure 9. (Color online) Lifetimes (a,b) and Current Densities (c,d) as a function of core size and temperature for both unstrained (left) and strained (right) conditions.

## ACKNOWLEDGMENTS

We thank Gerhard Klimeck and NCN/nanohub.org for providing NEMO3D for this research. Support was provided by the National Science Foundation (NSF) under Award No. DMR-0807232. Sandia is a multiprogram laboratory operated by Sandia Corporation, a Lockheed Martin Corporation, for the United States Department of Energy under Contract No. DEAC04-94AL85000.

## REFERENCES

- [1] Albo, A., Bahir, G., and Fekete, D., "Absorption of Terahertz Radiation in Ge/Si(001) Heterostructures with Quantum Dots," *JETP Letters* **92**(12), 793 – 798 (2010).
- [2] Albo, A., Bahir, G., and Fekete, D., "Improved hole confinement in thin double layer GaInAsN–GaAsSbN quantum well structure for telecom-wavelength lasers," *Journal of Applied Physics* **108**(9), 093116 (2010).
- [3] Asryan, L. V. and Luryi, S., "Temperature-insensitive semiconductor quantum dot laser," *Solid-State Electronics* **47**(2), 205 – 212 (2003).
- [4] Klimeck, G., Ahmed, S., Bae, H., Kharche, N., Clark, S., Haley, B., Sunhee, Naumov, M., Ryu, H., Saied, F., Prada, M., Korkusinski, Boykin, T. B., and Rahman, R., "Atomistic Simulation of Realistically Sized Nanodevices Using NEMO 3-D Part I– models and Benchmarks," *IEEE Transactions on Electron Devices* **54**(9), 2090 – 2099 (2007).
- [5] Balet, L. P., Ivanov, S. A., Piryatinski, A., Achermann, M., and Klimov, V. I., "Inverted Core/Shell Nanocrystals Continuously Tunable between Type-I and Type-II Localization Regimes," *Nano Letters* **4**(8), 1485 – 1488 (2004).
- [6] Boykin, T. B., Klimeck, G., and Oyafuso, F., "Valence band effective-mass expressions in the  $sp^3d^5s^*$  empirical tightbinding model applied to a Si and Ge parametrization," *Phys. Rev. B* **69**(11), 115201 (2004).
- [7] Usman, M., Heck, S., Clarke, E., Spencer, P., Ryu, H., Murray, R., and Klimeck, G., "Experimental and theoretical study of polarization-dependent optical transitions in InAs quantum dots at telecommunication-wavelengths (1300-1500 nm)," *Journal of Applied Physics* **109**(10), 104510 (2011).
- [8] Lee, S., Oyafuso, F., von Allmen, P., and Klimeck, G., "Boundary conditions for the electronic structure of finite-extent embedded semiconductor nanostructures," *Phys. Rev. B* **69**(4), 045316 (2004).
- [9] Rahman, R., Wellard, C. J., Bradbury, F. R., Prada, M., Cole, J. H., Klimeck, G., and Hollenberg, L. C. L., "High Precision Quantum Control of Single Donor Spins in Silicon," *Phys. Rev. Lett.* **99**(3), 036403 (2007).
- [10] Andreev, A. D. and O'Reilly, E. P., "Optical matrix element in InAs/GaAs quantum dots: Dependence on quantum dot parameters," *Applied Physics Letters* **87**, 213106 –213106–3 (nov 2005).

- [11] Schneider, H. and v. Klitzing, K., “Thermionic emission and Gaussian transport of holes in  $\text{GaAs}/\text{Al}_x\text{Ga}_{1-x}\text{As}$  multiple-quantum-well structure,” *Phys. Rev. B* **38**(9), 6160–6165 (1988).
- [12] Neupane, M. R., Lake, R. K., and Rahman, R., “Core size dependence of the confinement energies, barrier heights, and hole lifetimes in Ge–core/Si-shell nanocrystals,” *Journal of Applied Physics* **under review** (2011).
- [13] Shen, H.-Y., Zeng, R. R., Zhou, Y.-P., Yu, G. F., Huang, C.-H., Zeng, Z.-D., Zhang, W. J., and Ye, Q. J., “Simultaneous Multiple Wavelength Laser Action in Various Neodymium Host Crystals,” *IEEE Journal of Quantum Electronics* **27**(10), 2315 – 2318 (1991).
- [14] Zhao, D., Zhu, Y., Li, R., and Liu, J., “Transient processes in a Ge/Si hetero-nanocrystal p-channel memory,” *Solid-State Electronics* **50**(3), 362 – 366 (2006).
- [15] Niculescu, E. C. and Radu, A., “Tunneling time correction to the intersubband optical absorption in a THz laser-dressed  $\text{GaAs}/\text{Al}_x\text{Ga}_{1-x}\text{As}$  quantum well,” *Eur. Phys. J. B* **80**(1), 73 – 82 (2011).
- [16] Ozmen, A., Yakar, Y., Cakir, B., and Atav, U., “Computation of the oscillator strength and absorption coefficients for the intersubband transitions of the spherical quantum dot,” *Optics Communications* **282**(19), 3999 – 4004 (2009).
- [17] Tkach, N. and Sety, Y., “Properties of the electron spectrum of a closed two-well spherical quantum dot and evolution of the spectrum with the outer-well width,” *Semiconductors* **40**, 1083–1092 (2006).
- [18] Kosti, R. and Stojanovic, D., “Nonlinear absorption spectra for intersubband transitions of  $\text{CdSe}/\text{ZnS}$  spherical quantum dots,” *Journal of Nanophotonics* **5**(1), 051810 (2011).